NANO LETTERS

Letter

pubs.acs.org/NanoLett

High-Efficiency Electrochemical Hydrogen Evolution Based on Surface Autocatalytic Effect of Ultrathin 3C-SiC Nanocrystals

Chengyu He,[†] Xinglong Wu,[†,*] Jiancang Shen,[†] and Paul K. Chu[‡,*]

[†]National Laboratory of Solid State Microstructures and Department of Physics, Nanjing University, Nanjing 210093, People's Republic of China

[‡]Department of Physics and Materials Science, City University of Hong Kong, Hong Kong, China

Supporting Information

ABSTRACT: Good understanding of the reaction mechanism in the electrochemical reduction of water to hydrogen is crucial to renewable energy technologies. Although previous studies have revealed that the surface properties of materials affect the catalytic reactivity, the effects of a catalytic surface on the hydrogen evolution reaction (HER) on the molecular level are still not well understood. Contrary to general belief, water molecules do not adsorb onto the surfaces of 3C-SiC nanocrystals (NCs), but rather spontaneously dissociate via a surface autocatalytic process forming a complex consisting of −H and −OH fragments. In this study, we show that ultrathin 3C-SiC NCs possess superior electrocatalytic activity in the HER. This arises from the large reduction in the activation barrier on the NC surface enabling efficient dissociation of H_2O molecules. Furthermore, the ultrathin 3C-SiC NCs show enhanced HER activity in photoelectrochemical cells and are very promising to the water splitting based on the synergistic electrocatalytic and photoelectrochemical actions. This study provides a molecular-level understanding of the HER mechanism and reveals that NCs with surface autocatalytic effects can be used to split water with high efficiency thereby enabling renewable and economical production of hydrogen.

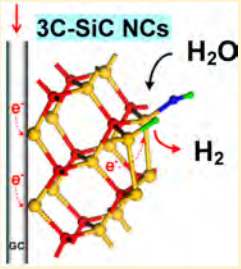

KEYWORDS: *3C-SiC nanocrystals, surface autocatalytic effect, water splitting, hydrogen evolution reaction*

Hydrogen is a green energy carrier having a high energy capacity.[1] Since hydrogen production from water splitting has large potential in renewable energy production,[2,3] there has been much research effort in identifying materials with efficient electrocatalytic and photoelectrochemical water splitting capability.[4−12] However, in order to identify and develop the proper catalysts, better understanding of the hydrogen evolution reaction (HER) mechanism is crucial. The interactions between solid surfaces and water molecules should be the driving force to accelerate HER and previous studies have revealed that the surface properties of catalysts affects the reactivity.[13,14] Nevertheless, despite past studies the effects of a catalytic surface on the HER on the molecular level are still not well understood. Recently, the interaction between water and solid surfaces has attracted increasing interests on account of potential applications to many areas such as heterogeneous catalysis, electrochemistry, and corrosion processes.[15] Contrary to general belief, water molecules do not adsorb onto the surfaces of certain solid materials, but instead dissociate via a surface autocatalytic process forming a complex consisting of −H and −OH species.[16−19] In this regard, it should be feasible to develop an advanced catalyst for high-efficiency electrochemical hydrogen evolution from direct water splitting based on the surface autocatalytic effect.

In our previous studies on the interaction between water and nanocrystal (NC) surfaces, we demonstrated that ultrathin 3C-SiC nanocrystals (NCs) can dissociate adsorbed H_2O molecules via a surface autocatalytic process forming a complex consisting of −H and −OH fragments by photoluminescence (PL) spectral identification.[20] The first-principle calculation suggests that the modified Si-terminated surface on the 3C-SiC NCs with −OH on one end of the Si−Si dimer and −H on the other end can break down H_2O molecules. This may be a suitable approach to produce hydrogen from direct water decomposition based on the surface autocatalytic effect of ultrathin SiC materials. In the work reported in this Letter, 3C-SiC NCs are used as an electrochemical catalyst in the HER, and ultrathin 3C-SiC NCs are observed to deliver superior performance under weakly acidic conditions. However, larger commercial 3C-SiC NCs about 20 nm in size do not show the same effects providing experimental evidence of the size dependence of the surface autocatalytic activity. Furthermore, 3C-SiC NCs supported on glassy carbon (GC) substrate serving as a photocathode exhibit enhanced HER activity compared to that in the dark thereby suggesting its potential use in photoelectrochemical cells. This study provides a molecular level understanding of the HER mechanism and particularly demonstrates important applications of NCs with surface autocatalytic effects in high-efficiency water splitting for renewable and economical production of hydrogen.

The detailed procedures to prepare the water suspension with ultrathin 3C-SiC NCs can be found elsewhere.[21] Succinctly speaking, about 6.0 g of 3C-SiC powders with a grain size of several micrometers were used as the precursor. An etching solution composed of 15 mL of 65 wt % nitric acid

Received: December 13, 2011
Published: March 2, 2012

(HNO_3) and 45 mL of 40 wt % hydrofluoric acid (HF) was used to etch the SiC powders at 100 °C for 1 h. The solution was cooled and centrifuged at 8000 rpm for 5 min to remove excess acid. The powders were washed with deionized water, dried at 70 °C for several hours, added to 30 mL of deionized water, ultrasonically treated for about 60 min, and finally centrifuged at 8000−10000 rpm for 10 min. The supernatant contained 3C-SiC NCs smaller than 8 nm in size. The morphology of the NCs was examined by high-resolution transmission electron microscopy (HR-TEM; JEM-2010, 200 kV) and the NC size distribution was determined by a particle size analyzer (Malvern, Zetasizer Nano ZS).

Electrochemical measurements were performed at ~25 °C in a three-electrode cell connected to a CHI 660D workstation (CH Instrument) (Supporting Information, Figure S1). A GC substrate coated with the 3C-SiC NC film was used as the working electrode whereas Ag/AgCl (3 mol L^{-1} KCl-filled) and a platinum wire served as the reference and counter electrodes, respectively. A 0.5 mol L^{-1} Na_2SO_4 solution (pH = 6.0) was the electrolyte and 500 W Xe lamp served as the light source in the photoelectrochemical measurements. The thin film electrodes were prepared according to the following procedures. The aqueous suspension containing 3C-SiC NCs (15 mL) with a concentration of 1 mg mL^{-1} and 0.4 mL of 5 wt % Nafion solution was treated ultrasonically for about 30 min, cast onto a GC substrate, and dried at 70 °C to evaporate the solvent. The film morphology was characterized by scanning electron microscopy (SEM; Hitachi S-4800) and the thickness was measured by surface profilometry (Zeta Instruments, Zeta-20).

Figure 1a depicts the TEM image of the as-prepared 3C-SiC NCs that are nearly spherical and have diameters between 1.5 and 7.5 nm. The inset shows the HR-TEM image of one NC. This NC is highly crystalline and the lattice fringes correspond to the (111) plane of 3C-SiC. Figure 1b displays the histogram of the NC size distribution. The NCs exhibit an almost asymptotic centric distribution and the diameters of most NCs are between 3.0 and 4.5 nm. Figure 1c,d shows the TEM image and X-ray diffraction (XRD) pattern of commercial 3C-SiC NCs (purchased from Alfa Aesar) with a size of about 20 nm. The PL spectra are acquired from the as-fabricated and commercial 3C-SiC NCs in water suspensions at a pH of 5.5 using an excitation wavelength of 360 nm (Supporting Information, Figure S2). In addition to a blue band stemming from quantum confinement, the as-prepared 3C-SiC NCs show an additional PL band at 510 nm arising from structures induced by −H and −OH dissociated from water and attached to Si dimers on the NC surface.[20] In contrary, no emission can be observed from the commercial 3C-SiC NCs. It should be noted that the room-temperature PL is relatively weak due to the indirect bandgap of large 3C-SiC.

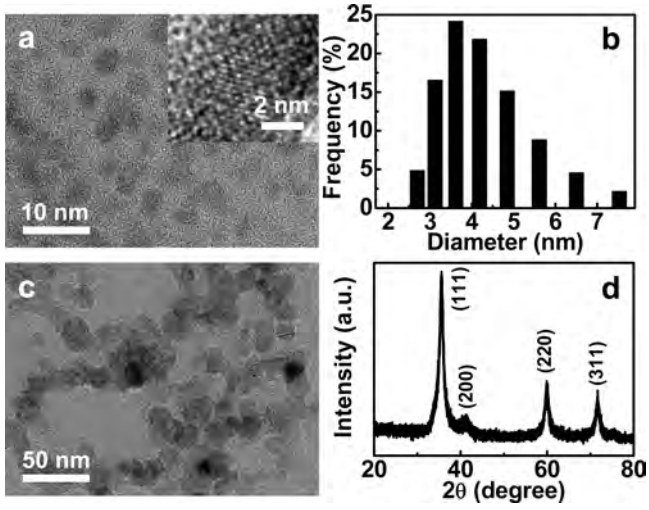

Figure 1. (a) TEM image of as-fabricated 3C-SiC NCs with the inset showing a typical high-resolution TEM image of a NC with lattice fringes corresponding to the (111) plane of 3C-SiC. (b) NC size distribution showing the most probable size of 3.6 nm. (c,d) TEM image (c) and XRD pattern (d) of commercial 3C-SiC NCs with a size of about 20 nm.

The ultrathin 3C-SiC NC film on the GC substrate consists of particles that have coalesced into a thin film (Figure 2) and the film thickness has the micrometer scale. The electrocatalytic HER activity of the film in a 0.5 mol L^{-1} Na_2SO_4 solution is determined using the three-electrode setup. Figure 3a shows the linear sweep voltammetry curves of the freshly prepared 3C-SiC NC film electrode (mean NC size of 3.6 nm) at different time (curves A−F) during consecutive measurements. In the first scan, the sample shows a small onset potential. The onset potential increases with time, as indicated by the shift to more negative potentials, and finally reaches a stable value. The increasing onset potential is caused by desorption of protons from the NC surface formed during chemical etching.[20] To evaluate the NC size dependence, several 3C-SiC NC film electrodes with different NC sizes are tested and the current−potential curve obtained from the electrode with a mean NC size of 3.0 nm is presented in Figure 3b. The final stable onset potentials are lower and electrocatalytic activity is higher. Similar experiments are performed on the commercial 3C-SiC NC film with similar catalyst loadings, but negligible currents are observed (Figure 3c). The results indicate that although large 3C-SiC NCs can also form −H and −OH groups on the surface,[16] the electrocatalytic activity is rather low and so the NC size plays an important role in the electrocatalytic HER activity. According to the stable polarization curves in Figure 3c, the ultrathin 3C-SiC NC film possesses far better electrocatalytic activity than the blank GC substrate. For comparison, the polarization curve is also obtained from a bare platinum foil electrode and the electrocatalytic activity of the ultrathin 3C-SiC NC sample is actually comparable to that of the platinum electrode. The current−time plot of the ultrathin

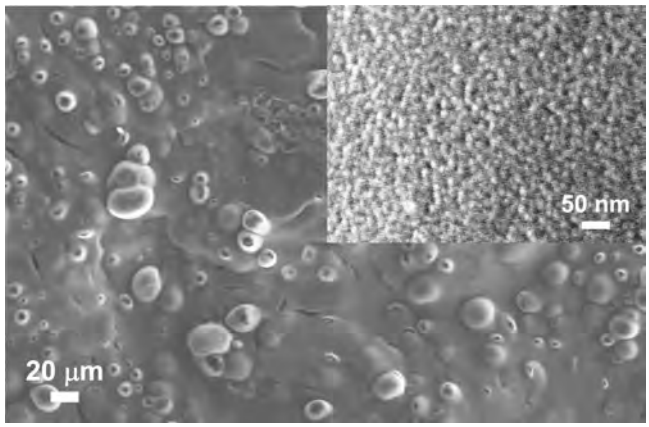

Figure 2. Representative SEM image of the ultrathin 3C-SiC NC film on a GC substrate. The inset shows the local enlargement.

dx.doi.org/10.1021/nl3006947 | Nano Lett. 2012, 12, 1545−1548

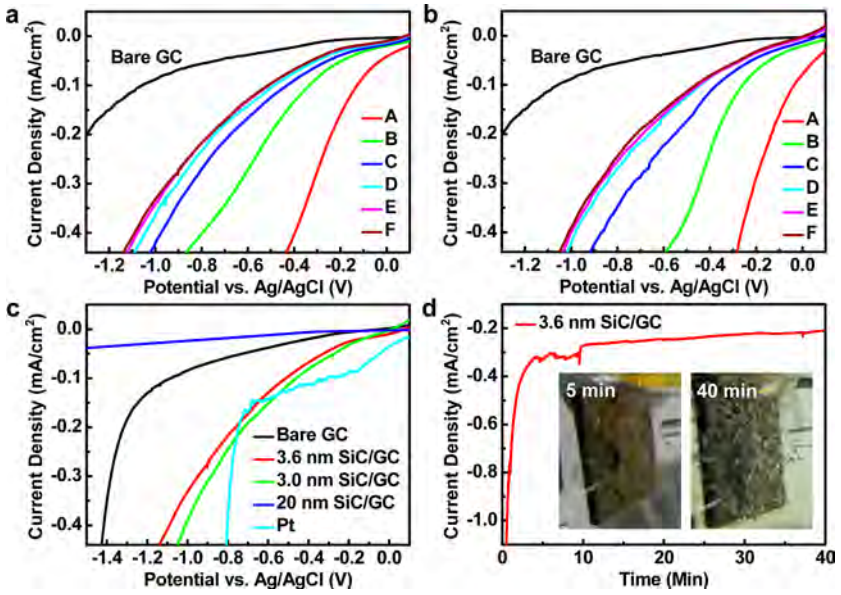

Figure 3. (a,b) Linear sweep voltammetry curves of the as-prepared nanocrystalline 3C-SiC electrode with NC sizes of 3.6 (a) and 3.0 nm (b) at different time (A–F) in consecutive measurements together with the data obtained from a blank GC substrate for comparison. (c) The stable polarization curves of the two 3C-SiC samples with different NC sizes on GC substrates. The corresponding results acquired from a commercial 3C-SiC sample with a NC size of about 20 nm and a bare Pt foil are also presented for reference. These curves are obtained from an aqueous 0.5 mol L^{-1} Na_2SO_4 solution (pH = 6.0) at a scanning rate of 10 mV s^{-1}. (d) Current–time plot of the ultrathin 3C-SiC NC film electrode at −0.8 V (vs Ag/AgCl) applied potential under the same conditions. The inset shows two digital pictures of the ultrathin 3C-SiC NC film electrode emitting hydrogen taken at different time during the amperometric *I–t* measurement. A small amount of bubbles can be seen nucleating on the electrode surface at the beginning and there are more bubbles on the surface as time elapses.

3C-SiC NC film electrode at −0.8 V applied potential (versus Ag/AgCl) is presented in Figure 3d. The stable current suggests that materials are durable in the HER. Bubbles can be clearly observed to evolve from the working electrode during the stability measurement (inset of Figure 3d and Figure S3 in Supporting Information). To clarify the role of pH, the electrocatalytic activity of the ultrathin 3C-SiC NCs obtained from the alkaline solution at a pH of 10.5 is determined (Supporting Information, Figure S4). Negligible electrocatalytic activity is observed suggesting that a specific surface H^+ concentration is necessary for the surface autocatalytic effect.[20]

To explain why ultrathin 3C-SiC NCs can accelerate hydrogen production, the mechanism is illustrated in Figure 4. When water molecules diffuse to a favorable dissociation site (Si-terminated surface) on the 3C-SiC NCs, they spontaneously split into two fragments (−H and −OH) bonded to two adjacent Si atoms (Si dimer).[20] This surface autocatalytic effect on the ultrathin 3C-SiC NCs reduces significantly the activation barrier for dissociation. Obviously, the smaller the NC size, the larger is the specific surface area and consequently, the higher the autocatalytic activity. Under favorable conditions, hydrogen atoms on the NC surface are reduced to produce hydrogen molecules when electrons are transferred from the electrode to −H. This hydrogen generation route has a lower activation barrier than that via direct water electrolysis. Finally, H_2O molecules adsorb and dissociate in this sustained dynamic process giving rise to efficient hydrogen production. Our experiments furnish evidence that the reaction can produce hydrogen continuously at room temperature especially under weakly acidic conditions. With regard to the NCs in a basic solution, −OH groups terminate the Si dangling bonds and so the NC surface cannot spontaneously break down water molecules. The weak autocatalytic effect subsequently leads to negligible electrocatalytic activity in the HER.

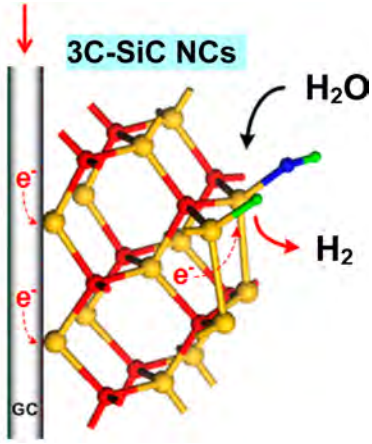

Figure 4. Schematic illustration of the mechanism governing the electrocatalytic HER on the ultrathin 3C-SiC/GC electrode. The 3C-SiC NC is indicated by the optimized structures of Si-terminated (001) surface where H_2O molecules dissociate forming a complex consisting of −H and −OH fragments. The big yellow balls and small red ones represent Si and C atoms, whereas the big blue balls and small green ones are O and H atoms, respectively.

As a semiconductor with proper band gap of 2.24 eV and flat band potential, high melting point, and good corrosion resistance in aqueous solutions, 3C-SiC is a suitable photocathode for water splitting.[22] As shown in Figure 5, the 3C-SiC NCs on the GC substrate exhibit enhanced HER activity compared to that in the dark,[23] whereas the corresponding change observed from the blank GC electrode is not noticeable.

Up to now, the most efficient catalysts for HER are platinum and other noble metals[24] but owing to the high costs cheaper alternative catalysts based on nonprecious metals and metal-

dx.doi.org/10.1021/nl3006947 | *Nano Lett.* 2012, 12, 1545–1548

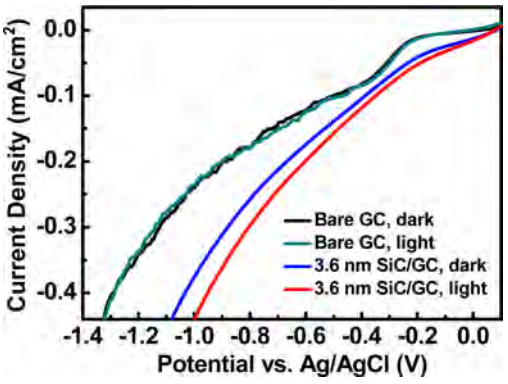

Figure 5. Current density versus potential curves determined from the two ultrathin 3C-SiC films on GC substrates in dark (blue) and under illumination (red). The corresponding results from the blank GC substrate are also displayed for comparison. These curves are obtained in an aqueous 0.5 mol L^{-1} Na_2SO_4 solution (pH = 6.0) at a scanning rate of 10 mV s^{-1}.

free materials are necessary for wider adoption. Despite past efforts, developing HER catalysts with high activity at lower costs remains a great challenge. Here, ultrathin 3C-SiC NCs with the surface autocatalytic effect are demonstrated to be excellent materials for efficient electrocatalytic hydrogen production. Given the abundance, low cost, and ease of fabrication, ultrathin 3C-SiC NCs are very promising high-performance electrocatalysts in energy conversion. The success of this approach suggests possible hydrogen production via water splitting on other materials such as ZnO and Fe_3O_4 that have similar surface autocatalytic activity.[17−19]

In conclusion, we report that ultrathin and nanoscale 3C-SiC NCs possess superior electrocatalytic activity in the HER due to the large reduction in the activation barrier of the NC surface to dissociate H_2O molecules. The ultrathin 3C-SiC NCs exhibit enhanced HER activity in photoelectrochemical cells and enable water splitting based on the synergistic electrocatalytic and photoelectrochemical actions. In addition to providing a molecular level understanding of the HER mechanism, this study reveals that NCs with surface autocatalytic effects can be used to split water with high efficiency enabling renewable and economical production of hydrogen.

■ ASSOCIATED CONTENT

Ⓢ Supporting Information

Photograph of the electrochemical cell, photoluminescence spectra of the samples, digital photographs of hydrogen bubbles, and electrocatalytic activity of ultrathin 3C-SiC NCs under alkaline conditions. This material is available free of charge via the Internet at http://pubs.acs.org.

■ AUTHOR INFORMATION

Corresponding Author

*E-mail: hkxlwu@nju.edu.cn (X.L.W); paul.chu@cityu.edu.hk (P.K.C.).

Notes

The authors declare no competing financial interest.

■ ACKNOWLEDGMENTS

This work was jointly supported by National Basic Research Program of China (2011CB922102), National Natural Science Foundation of China (60976063), PAPD and Jiangsu Planned Projects for Postdoctoral Research Funds (1102026C). Partial support was also provided by Hong Kong Research Grants Council (RGC) General Research Funds (GRF) (CityU 112510) and City University of Hong Kong Direct Allocation Grant 9360110.

■ REFERENCES

(1) Dresselhaus, M. S.; Thomas, I. L. *Nature* **2001**, *414*, 332−337.
(2) Lewis, N. S.; Nocera, D. G. *Proc. Natl. Acad. Sci. U.S.A.* **2006**, *103*, 15729−15735.
(3) Walter, M. G.; Warren, E. L.; McKone, J. R.; Boettcher, S. W.; Mi, Q.; Santori, E. A.; Lewis, N. S. *Chem. Rev.* **2010**, *110*, 6446−6473.
(4) Kanan, M. W.; Nocera, D. G. *Science* **2008**, *321*, 1072−1075.
(5) Li, Y. G.; Wang, H. L.; Xie, L. M.; Liang, Y. Y.; Hong, G. S.; Dai, H. J. *J. Am. Chem. Soc.* **2011**, *133*, 7296−7299.
(6) Yeo, B. S.; Bell, A. T. *J. Am. Chem. Soc.* **2011**, *133*, 5587−5593.
(7) Li, Y. G.; Hasin, P.; Wu, Y. Y. *Adv. Mater.* **2010**, *22*, 1926−1929.
(8) Hou, Y. D.; Abrams, B. L.; Vesborg, P. C. K.; Bjorketun, M. E.; Herbst, K.; Bech, L.; Setti, A. M.; Damsgaard, C. D.; Pedersen, T.; Hansen, O.; Rossmeisl, J.; Dahl, S.; Norskov, J. K.; Chorkendorff, I. *Nat. Mater.* **2011**, *10*, 434−438.
(9) Reece, S. Y.; Hamel, J. A.; Sung, K.; Jarvi, T. D.; Esswein, A. J.; Pijpers, J. J. H.; Nocera, D. G. *Science* **2011**, *334*, 645−648.
(10) Boettcher, S. W.; Warren, E. L.; Putnam, M. C.; Santori, E. A.; Turner-Evans, D.; Kelzenberg, M. D.; Walter, M. G.; McKone, J. R.; Brunschwig, B. S.; Atwater, H. A.; Lewis, N. S. *J. Am. Chem. Soc.* **2011**, *133*, 1216−1219.
(11) Roy, P.; Das, C.; Lee, K.; Hahn, R.; Ruff, T.; Moll, M.; Schmuki, P. *J. Am. Chem. Soc.* **2011**, *133*, 5629−5631.
(12) Paracchino, A.; Laporte, V.; Sivula, K.; Gratzel, M.; Thimsen, E. *Nat. Mater.* **2011**, *10*, 456−461.
(13) Jaramillo, T. F.; Jorgensen, K. P.; Bonde, J.; Nielsen, J. H.; Horch, S.; Chorkendorff, I. *Science* **2007**, *317*, 100−102.
(14) Subbaraman, R.; Tripkovic, D.; Strmcnik, D.; Chang, K. C.; Uchimura, M.; Paulikas, A. P.; Stamenkovic, V.; Markovic, N. M. *Science* **2011**, *334*, 1256−1260.
(15) Henderson, M. A. *Surf. Sci. Rep.* **2002**, *46*, 1−308.
(16) Cicero, G.; Catellani, A.; Galli, G. *Phys. Rev. Lett.* **2004**, *93*, 016102.
(17) Meyer, B.; Marx, D.; Dulub, O.; Diebold, U.; Kunat, M.; Langenberg, D.; Woll, C. *Angew. Chem., Int. Ed.* **2004**, *43*, 6642−6645.
(18) Dulub, O.; Meyer, B.; Diebold, U. *Phys. Rev. Lett.* **2005**, *95*, 136101.
(19) Parkinson, G. S.; Novotny, Z.; Jacobson, P.; Schmid, M.; Diebold, U. *J. Am. Chem. Soc.* **2011**, *133*, 12650−12655.
(20) Wu, X. L.; Xiong, S. J.; Zhu, J.; Wang, J.; Shen, J. C.; Chu, P. K. *Nano Lett.* **2009**, *9*, 4053−4060.
(21) Zhu, J.; Liu, Z.; Wu, X. L.; Xu, L. L.; Zhang, W. C.; Chu, P. K. *Nanotechnology* **2007**, *18*, 365603.
(22) van Dorp, D. H.; Hijnen, N.; Di Vece, M.; Kelly, J. J. *Angew. Chem., Int. Ed.* **2009**, *48*, 6085−6088.
(23) Wu, X. L.; Fan, J. Y.; Qiu, T.; Yang, X.; Siu, G. G.; Chu, P. K. *Phys. Rev. Lett.* **2005**, *94*, 026102.
(24) Bockris, J. O'M.; Reddy, A. K. N.; Gamboa-Aldeco, M. *Modern Electrochemistry 2A*, 2nd ed.; Kluwer Academic/Plenum Publishers: New York, 1998.

Supporting Information

High-Efficiency Electrochemical Hydrogen Evolution Based on Surface Autocatalytic Effect of Ultrathin 3C-SiC Nanocrystals

Chengyu He, Xinglong Wu,* Jiancang Shen, and Paul K. Chu*

Figure S1. Photograph of the electrochemical cell composed of three chambers. The anode and cathode electrodes are immersed in separate cells divided by a Nafion 117 film and a Luggin capillary separates the working compartment from the reference compartment. An Ag/AgCl electrode in 3 mol L^{-1} KCl solution (with a nominal potential of 0.210 V versus reversible hydrogen electrode) and a platinum wire are used as the reference and counter electrodes, respectively. The working electrode is a 2 cm × 1.5 cm glassy carbon (GC) substrate modified with catalysts. Typically, a 1.5 cm × 1.5 cm substrate is immersed in the solution. The electrolyte is purged with N_2 for 30 min to eliminate dissolved gases such as O_2 before measurements.

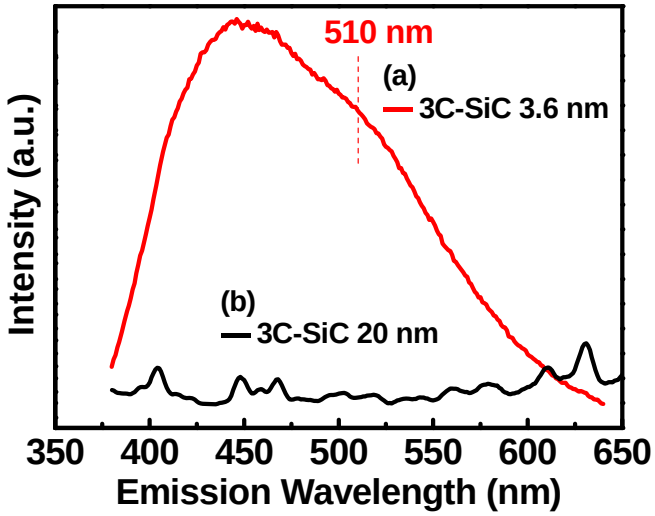

Figure S2. Photoluminescence (PL) spectra of the water suspensions (pH = 5.5) of two 3C-SiC nanocrystals acquired at an excitation wavelength of 360 nm: (a) As-prepared 3C-SiC nanocrystal with the most probable size of 3.6 nm and (b) Commercial nanocrystals with a size of about 20 nm. From the ultrathin 3C-SiC nanocrystal suspension, an evident green shoulder at 510 nm from –H and –OH bonding at the Si-terminated nanocrystal surface can be observed in addition to the blue PL band at 450 nm due to quantum confinement (Ref. 20). This green band is a fingerprint to identify the surface autocatalytic effect of small size 3C-SiC nanocrystals. It vanishes when the 3C-SiC nanocrystals have a size of about 20 nm suggesting disappearance of the surface autocatalytic effect.

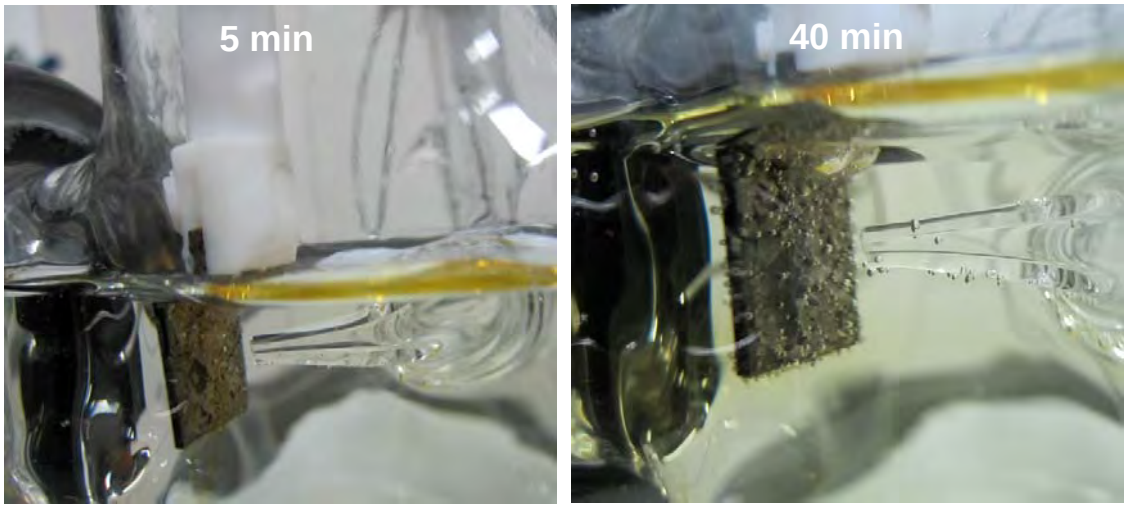

Figure S3. Two digital photographs shows electrochemical hydrogen evolution in the cell at –0.8 V (versus Ag/AgCl) applied potential. The two pictures are photographed at 5 min and 40 min, respectively, during the amperometric *I* - *t* measurement described in the text.

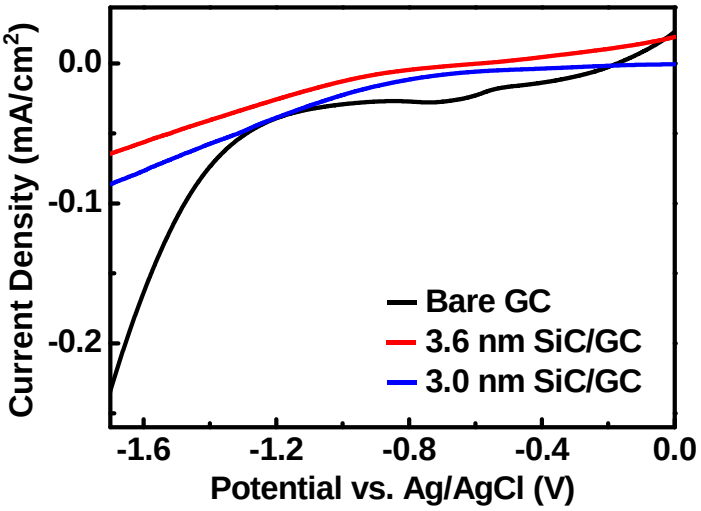

Figure S4. Linear sweep voltammetry curves of the two GC substrate electrodes coated with the ultrathin 3C-SiC NCs obtained from the alkaline suspensions (pH adjusted to 10.5 by NaOH) as well as blank GC electrode, recorded in an aqueous 0.0001 mol L^{-1} NaOH solution.